Research Article
Volume 13:4, 2023

Journal of Blood and lymph

ISSN: 2165-7831

Open Access

TM4SF1 is Essential for Embryonic Blood Vessel Development

Chi-Iou Lin[1^], Anne Merley[1,2^], Hiromi Wada[1,3], Jianwei Zheng[1,4] and Shou-Ching S. Jaminet[1,5*]

[1]*Department of Pathology, Beth Israel Deaconess Medical Center and Harvard Medical School, Boston, MA, United States of America*

[2]*Department of Center for Animal Resources and Education, Brown University, Providence, RI, United States of America*

[3]*Department of Isotope Science Center, The University of Tokyo, Tokyo, Japan*

[4]*Department of General Surgery, TianTan Hospital, Beijing, China*

[5]*Angiex Inc, Cambridge, MA, United States of America*

^ Co- first author

Abstract

Transmembrane-4 L-Six Family Member-1 (TmM4SF1) is a small cell surface glycoprotein that is highly and selectively expressed on endothelial cells and mesenchymal stem cells. TM4SF1 regulates cellular functions by forming protein complexes called TMED (TM4SF1-enriched micro domains) that internalize via microtubules from the cell surface and transport recruited proteins to intracellular locations including the nucleus. Through a genetically manipulated mouse model, we demonstrate here that TM4SF1 is essential for blood vessel development. *Tm4sf1* null embryos fail to develop blood vessels and experience lethality at E9.5. *Tm4sf1* heterozygous embryos are smaller in body size during early embryonic development, and almost half die in utero due to intracranial hemorrhage in the intraventricular and subarachnoid space which becomes apparent by E17.5. Surviving *Tm4sf1* heterozygotes do not display overt phenotypic differences relative to wild type littermates postnatally. Together these studies demonstrate that TM4SF1, through its molecular facilitator role in TMED, intimately regulates blood vessel formation during embryonic development.

Keywords: TM4SF1 • Endothelial cell • Mesenchymal stem cell • Knockout mice • Blood vessel development • Intraventricular and subarachnoid hemorrhage

Introduction

Transmembrane-4 L-Six Family Member-1 (TM4SF1) is a small plasma membrane glycoprotein of tetraspanin *topology* but distinct *homology* from the thirty-three genuine tetraspanins [1]. TM4SF1 was originally discovered as a tumor-associated antigen [2] that is also expressed at low levels by normal vascular endothelium [3-5]. Subsequently, we demonstrated that TM4SF1 is expressed at high levels in cultured Endothelial Cells (ECs) originating from blood or lymphatic vessels [5,6] endothelial progenitor cells and in bone marrow-derived Mesenchymal Stem Cells (MSCs) [7] and *in vivo* in endothelium undergoing pathological angiogenesis in both experimental models of angiogenesis in mice [5] and in human cancers [5,4]. Our studies further demonstrated that depletion of TM4SF1 in ECs through knockdown (i) prevents the cellular polarization necessary for EC migration and proliferation *in vitro*; [5,6] (ii) blocks intercellular interactions and junction formation in cultured ECs and (iii) inhibits vessel maturation in pathological angiogenesis *in vivo* [5].

TM4SF1 regulates biological and cellular activities through its ability to form 100-300 nm diameter protein complexes called TMED (TM4SF1-enriched micro domains) on the surfaces of cells that express high levels of TM4SF1 *in vitro* [4-7] and the tumor endothelium of human cancers *in vivo* [4]. Each TMED contains three to fourteen TM4SF1 molecules and functions as a membrane dock that recruits membrane proteins primarily laterally through the transmembrane domains, and bring along their intracellular membrane-proximal signaling components [4,6]. Through a novel and as yet unelucidated mechanism, TMED internalize from the cell surface *via* microtubules with an ultimate destination in the nuclear compartment [4] and distribute recruited proteins from the plasma membrane to intracellular locations. TMED also facilitate the adhesion of ECs to matrix by recruiting integrin-$\alpha5\beta1$ [5]. This process enables the formation of nanopodia: Thin, long membrane-lined channels within which actin microfilaments extend and/or retract during cell movement and which facilitate the homotypic and heterotypic intercellular interactions for stable vessel formation [5-8].

In this study, we investigated TM4SF1's functional role in normal blood vessel development using a knockout strategy in mice. We report that *Tm4sf1* null embryos fail to form blood vessels and experience embryonic lethality at E9.5; heterozygotes are smaller in size than wild type embryos during early embryonic growth, and half die in utero, often with intraventricular and subarachnoid hemorrhage. The half of *Tm4sf1* -heterozygous pups born alive are fertile with normal physiological functions. Together these studies reveal that TM4SF1, through its ability to form TMED and internalize to intracellular space, intimately regulates blood vessel formation during embryonic development.

Materials and Methods

Anti-TM4SF1 antibodies

Anti-TM4SF1 antibodies were the same as used in our earlier studies: (1) The anti-mouse TM4SF1 antibody 2A7A (a chimeric antibody with the variable region of a rabbit anti-mouse TM4SF1 monoclonal antibody and the constant region of a human IgG1) [9] and (2) The anti-human TM4SF1 antibody 8G4 (IgG1, mouse monoclonal [8]; Millipore Sigma (Burlington MA), catalog number MABC1723).

Cells and cell culture

All nine human primary cells, HUVEC (Human Umbilical Vein Endothelial Cells), HLMEC (Human Lung Microvascular Endothelial Cells), HDMEC, (Human Dermal Microvascular Endothelial Cells), HCAEC (Human

***Corresponding Author:** Dr. Shou-Ching S. Jaminet, Angiex Inc, Cambridge, MA, United States of America; Email: scj@jaminetlab.com*

Received: 19-Sep-2023, Manuscript No. JBL-23-114116; **Editor assigned:** 22-Sep-2023, PreQC No. JBL-23-114116(PQ); **Reviewed:** 06-Oct-2023, QC No. JBL-23-114116; **Revised:** 13-Oct-2023, Manuscript No. JBL-23-114116 (R); **Published:** 20-Oct-2023, DOI: 10.37421/2165-7831.2023.13.310

Coronary Artery Endothelial Cells), HPAEC (Human Pulmonary Artery Endothelial Cells), ECFC (Endothelial Colony Forming Cells), HMVEC-dLy (Human Dermal Microvascular Lymphatic Endothelial Cells), HBdSMC (Human Bladder Smooth Muscle Cells, HDF (Human Dermal Fibroblasts), HEMa-LP (Human Epidermal Melanocytes, adult) were purchased along with their respective media from Lonza (Walkersville, MD) and used within six passages in all experiments conducted in this study. Three cell lines, 3T3 (fibroblast, mouse embryo), HEK393 (Human Embryonic Kidney Cells), and MS1 (Mouse SV1 Immortalized Islet Endothelial Cells) were acquired from ATCC (American Type Culture Collection, Gaithersburg, MD) cultured in their respective media suggested by ATCC, and used within five passages after being awakened from liquid nitrogen. Leukocytes either human or mouse, were isolated from fresh blood.

Flow cytometry

Experimental procedures were described in detail previously [8]. Briefly, 1 × 10^6 freshly harvested cells (HPAEC, HDF, and HEK293) were washed in cold PBS, suspended in 1 ml cold blocking buffer (PBS/2%FBS) that contained 100 ng 1st antibody 8G4 or mouse IgG1 (Sigma, Saint Louis, MO) and incubated at 4°C for 30 min with occasional agitation. Cells were centrifuged (500 xg for 5 min), followed by 100 ng/ml 2nd antibody (Alexa-488 labeled donkey anti-human or mouse IgG; ThermoFisher, Waltham, MA) for another 30 min at 4°C with washing 3x with cold PBS in between the incubations. Cell suspensions were analyzed with FACScan (Becton Dickinson, San Jose CA). 10^4 events were collected for each analysis.

Generation of *Tm4sf1* knockout mice

To generate the *Tm4sf1* knockout mice, we (1) produced the linearized *Tm4sf1* genome targeting construct pM253/PUH-PDH/Neo (8,461 bp), (2) introduced the construct into embryonic stem cells (ESCs) as described below, (3) identified mouse W4/129S6 ESCs that had TM4SF1 genome Ex3 to Ex5 targeted and replaced with loxP-Neo-loxP through homologous recombination, and (4) implanted the ESC clones into Fv129 mice (Charles River Laboratory, Shrewsbury, MA). A schematic summary of the generation of the knockout mice is detailed in Figure 2. All PCR primers used in TM4SF1 knockout mice are listed in supplementary material Table S1.

RP24-402K15 chloramphenicol resistant Bac clone that contains mouse TM4SF1 locus (acquired from NIH) was used as the source of mouse TM4SF1 genomic sequence. Four constructs were made to generate a *Tm4sf1* gene targeting construct: (i) pM253/UH-DH (5.7 kb) plasmid. PCR amplified UH (657 bp; 5' Ex3 flanking region) and DH (634 bp; reside in intron 6) DNA fragments from RP24-402K15, cut with Xba1 and ligated to generate UH-DH, followed by Kpn1 and HindIII cut for insertion into the pM253 vector (provided by Dr. W.C. Aird) to produce pM253/UH-DH (ampicillin resistant). (ii) pM253/UH-HR-DH (13.5 kb) gene repair vector. pM253/UH-DH plasmid was linearized and UH-DH arms separated through an Xba1 cut and electroporated into RP24-402K15/EL-250 bacteria for homologous recombination (HR) to bring in TM4SF1 Ex3 to Ex6 (9,013 bp) genome segment to the plasmid. The plasmid was confirmed *via* PCR through UP and DP primer sets. (iii) PUH/loxP-Neo-loxP/PDH (2.85 kb) cassette. PCR amplified the PUH (463 bp; 5' Ex3 flanking region adjacent to Ex3) and PDH (587 bp; 3' Ex5 intron region) DNA fragments from RP24-402K15, respectively cut with Bsa1 and BsmB1 and inserted on either side of the loxP-Neo-loxP cassette. (iv) pM253/PUH/loxP-Neo-loxP/PDH (12.9 kb) targeting plasmid. RP24-402K15/EL-250 bacteria that contain pM253/UH-HR-DH gene repair vector was transfected with PUH/loxP-Neo-loxP/PDH cassette to generate pM253/PUH/loxP-Neo-loxP/PDH plasmid through HR (neomycin resistant). The removal of 2,345 bp long Ex3 to Ex5 was then confirmed via PCR using TM-UPH-Neo forward and reverse primers. The 8,461 bp targeting construct was then released via Kpn1 and HindIII cut and transfected W4/129S6 ESCs (Taconic Biosciences, Albany, NY). G418 antibiotic (ThermoFisher) selection at 350 ug/ml was initiated 24 hours following targeting and neomycin-resistant ESC clones were screened for successful homologous recombination with PCR using the genotyping primer sets.

The Institutional Animal Care and Use Committee at Beth Israel Deaconess Medical Center, Boston, approved all animal experiments (protocol #100-2011). Positive *Tm4sf1* -/+ ES clones were amplified and submitted to the BIDMC transgenic core facility for injection into blastocysts. Briefly, targeted ESC clones were microinjected into C57BL/6-derived blastocyst stage embryos which were then transplanted into the uteri of recipient C57BL/6 females (Charles River Laboratory) to generate chimeric mice. Resulting chimeric males were bred with C57BL/6 females to obtain mice heterozygous for the inactivated loci. The heterozygous F1 male were back-crossed with C57BL/6 females to generate F2 heterozygous male and repeated for 8 generations to stabilize the chromosome before conducting the TM4SF1 heterozygotes male and female inbred mating to obtain homozygous embryos.

PCR genotyping

Genotyping was conducted using chromosomal DNA extracted from either yolk sac or a 2 mm tail clip from P14 to P21 postnatal mice. PCR analyses were performed with primers specific for the wild-type and targeted alleles. Tissues were submerged in gitschier buffer in the presence of B-mercaptoethanol and proteinase K to release chromosomal DNA. PCR conditions as described by the manufacturer of ampli taq polymerase (Perkin-Elmer Cetus, Norwalk, CT) were used to generate fragments from wild-type (596 bp) and targeted (397 bp) alleles on 1% agarose gels.

Multi-Gene Transcriptional Profiling (MGTP) approach to quantitative real-time PCR (qPCR)

MGTP is a qPCR technique that efficiently quantifies mRNA copies per cell and performed by MGTP core. Total RNA was prepared using the RNeasy kit with DNase-I treatment (Qiagen, Chatsworth, CA) and cDNA using random primers and SuperScript III (ThermoFisher). Human aorta and vein total RNA were purchased from biochain (Newark, CA). For each data point, mean ± SD were calculated from three different samples from three separate experiments. PCR reactions for each cDNA sample were performed in duplicate. Transcript abundances were normalized/10^6 18S-rRNA copies to approximate number of transcripts/cell [10]. All MGTP primer sequences used in the study were listed in Supplementary material Table S2.

Mouse organ harvest and ImmunoHistoChemical (IHC) staining

Experimental procedures were described in detail in previous studies [11]. Briefly, mouse tissues were immediately placed in 4% Paraformaldehyde(PFA) after harvesting from 8 weeks old C57BL/6 mice, and cryostat sections were immunostained with anti-mouse *Tm4sf1* antibody 2A7A followed by donkey anti-human HRP-conjugated secondary antibodies (ThermoFisher). Normal human liver section was prepared from surgically removed liver transplant by Dr. Lawrence Brown at BIDMC's Pathology Department and placed in 4% paraformaldehyde followed by OCT (Optimal cutting temperature) mounting and cryostat sectioning for staining with mouse anti-human TM4SF1 antibody 8G4 with subsequent anti-mouse HRP-conjugated 2nd antibodies (ThermoFisher). All IHC images were representative selections from at least three separate sections and were taken by Dr. Harold Dvorak. For whole mount mouse embryo and retina staining, Alexa488-conjugated 2A7A was used and captured images *via* keyence BZ-9000E microscope (Itasca, IL).

Embryo images, videos and immunostaining

All bright field images or videos of embryos harvested from different developmental stages were taken from live cam attached Wild photo mikroskop M400, Stereo photomicroscope (Martin Microscope, SC). Wholemount staining was carried out as described [12]. Briefly, E9.5 embryos were fixed 4 hours in 4% PFA in PBS at 4°C, rinsed in PBST (0.1% Tween-20/PBS), and incubated with Alexa488-conjugated anti-mouse TM4SF1 antibody 2A7A in blocking buffer (PBST/2% FBS) for two nights at 4°C. Fluorescence images were then acquired *via* Keyence microscope after thoroughly washing the embryos in PBST for overnight at 4°C. For Tm4s1 histology staining, 4% PFA fixed embryos were cryoprotected overnight in 20% sucrose/PBS, embedded in OCT (Tissue-Tek), sectioned (6 μm) and stained with the 2A7A antibody followed by HRP-conjugated anti-human 2nd antibody and Eosin counterstaining. For H and E staining, embryos were preserved in 50% ethanol before being processed for

FFPE for H and E staining at BIDMC's tissue processing core.

Results

TM4SF1 expression is largely limited to ECs *in vitro* and *in vivo*

We surveyed TM4SF1 expression in cultured ECs and six non-EC and non-tumor cell types that originated from both human and mouse tissues. qPCR revealed that human TM4SF1 expression in non-ECs was either very low as in smooth muscle cells (HBdSMC, bladder) and fibroblast (HDF, dermal), or was not detectably expressed as in kidney epithelial cells (HEK293), epidermal melanocytes (HemaLP), and White Blood Cells (WBC) (Figure S1). TM4SF1 expression in cells of mouse origin such as MS1 (SV40-immortalized mouse islet EC), 3T3 (embryonic fibroblasts) and mWBC was consonant with TM4SF1 expression in the corresponding human cell lineages (Figure S1A).

IHC staining in tissue sections prepared from six different mouse tissues (liver, lung, heart, kidney, brain, and retina) provided further evidence that TM4SF1 expression was limited to vascular endothelium, and that expression was highest in the endothelium of arteries, followed by veins and capillaries Figure 1A. Strong TM4SF1 expression is also seen in kidney glomeruli and in the choroid plexus epithelium of the lateral ventricle as well as the subependymal cell layer in the mouse brain (Figure 1A). Similar TM4SF1 localization was demonstrated in both mouse and human tissues; for example, the human liver exhibits arterial>venous>capillary endothelial staining (Figure 1B). In agreement, qPCR demonstrated that TM4SF1 gene expression in RNA from human aorta was 4.8-fold greater than that from pulmonary vein ($p=0.0026$) (Figure 1C).

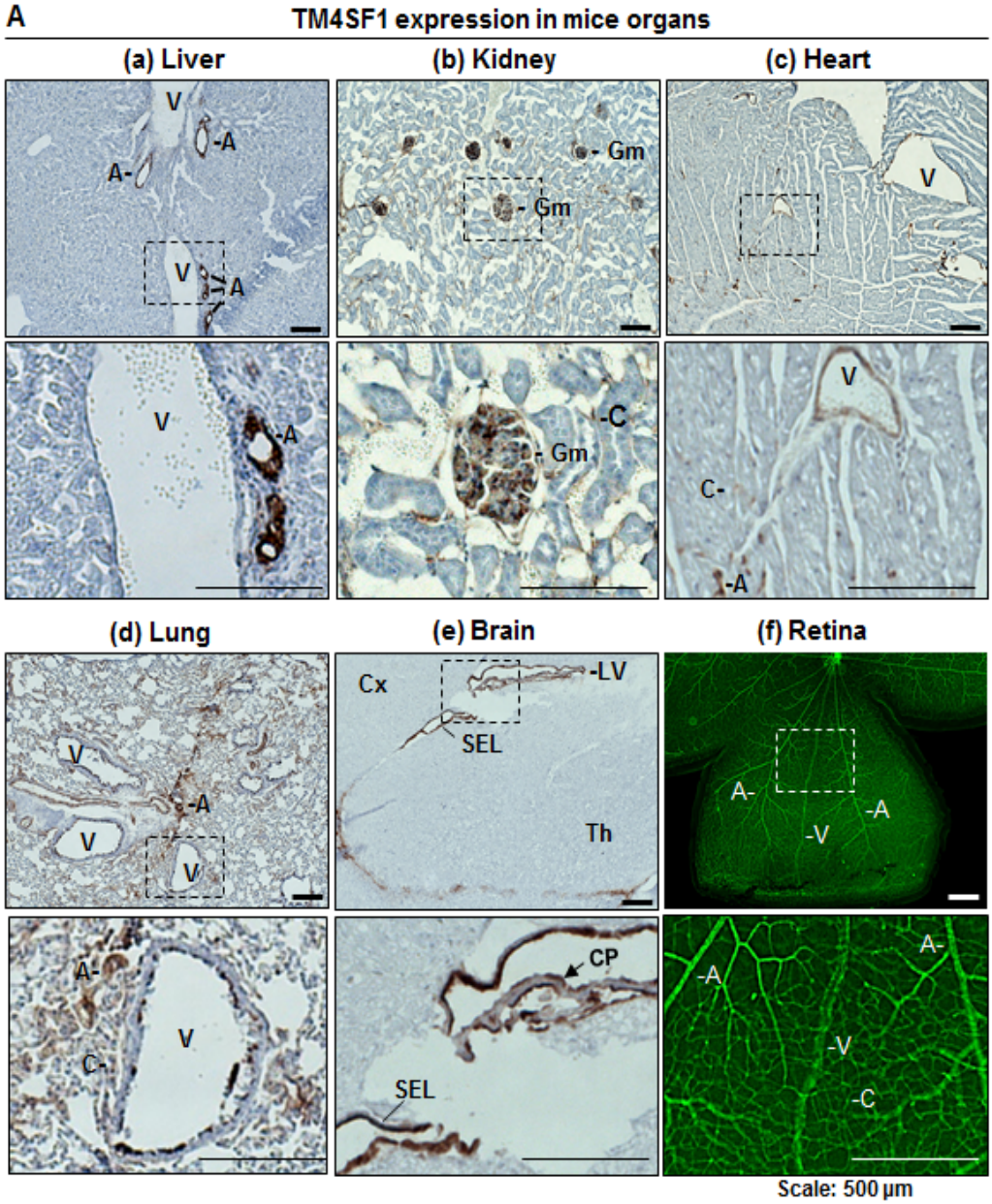

Figure 1A. TM4SF1 expression in the endothelium of mouse tissues *in vivo*. TM4SF1 IHC staining with HRP-conjugated 2nd antibody and eosin was conducted in tissue sections prepared from 8-week-old C57BL/6 mouse organs; (a) liver, (b) kidney, (c) heart, (d) lung, and (e) brain. (f) Day-18 C57BL/6 mouse retina wholemount staining with Alexa488-conjugated anti-mouse TM4SF1 antibody 2A7A. Representative IHC staining showed that TM4SF1 expression was largely limited to blood vessels with a tendency for the highest TM4SF1 expression to be in arteries (A), intermediate expression in veins (V), and the lowest expression in capillaries (C). Positive TM4SF1 expression was also seen in kidney glomeruli (Gm) and in the choroid plexus (CP; black arrow) epithelium of lateral ventricles (LV) along with the subependymal cell layer (SEL) in brain; no expression was observed in cortex (Cx) and thalamus (Th).

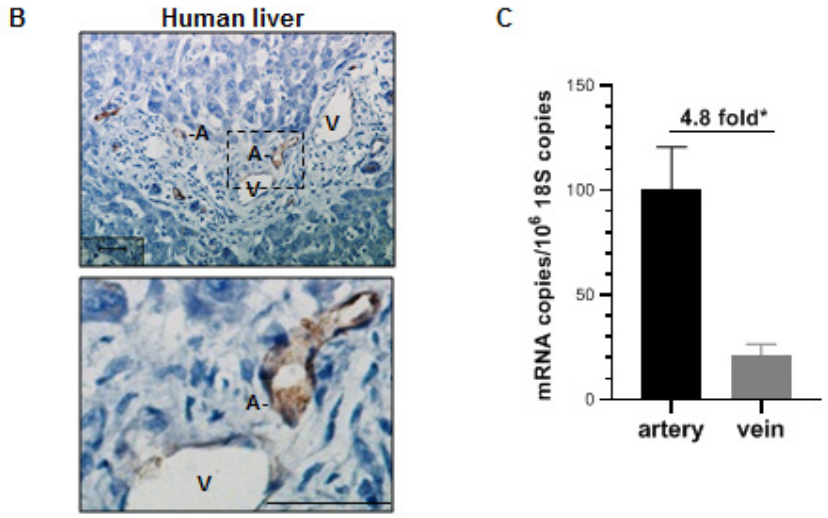

Figure 1B and 1C. TM4SF1 expression in the endothelium of human tissues *in vivo* . (B) Representative IHC staining in human liver section revealed that TM4SF1 expression was largely limited to blood vessels with a tendency for the higher TM4SF1 expression in arteries (A) than in veins (C). (C) qPCR using total RNA acquired from three different human aorta and pulmonary vein samples showed TM4SF1 expression was 4.8-fold higher in artery than vein (p=0.0026).

Tm4sf1 -knockout mice are embryonic lethal at embryonic day-9.5 (E9.5)

The mouse *Tm4sf1* gene is encoded on the minus strand of chromosome-3 from nucleotides 57,105,910 to 57,089,531. It contains seven Exons (Ex); the protein coding region begins in Ex3 and ends in Ex7, and encodes 202 amino acids (Figure S2A). We used standard gene targeting strategies to generate *Tm4sf1* -knockout mice; *Tm4sf1's* first three coding exons (Ex3 to Ex5) start with an initiation codon ATG, and our targeting strategy was designed to completely eliminate TM4SF1 protein translation by deleting Ex3 to EX5 (Figure S2B).

Genotypes of progeny of intercrossed *Tm4sf1* -heterozygous mice from E9.5 to Weaning Age (WA) (postnatal day-14 to day-21) are presented in Table 1. At WA, 154 pups were accounted to 30 litters, 74 pups were heterozygous (+/-), 80 were wild type (+/+), and 0 were knockout (-/-). The ratio of +/- to +/+ was 0.93 at WA, substantially different from the expected Mendelian ratio of 2, and the 5.1 pups/litter was also below the normal average of 8 pups/litter. These results indicate that all *Tm4sf1* -knockout mice died in utero; and that of the *Tm4sf1* -heterozygous, (1) Working from expected litter size, only 74 of an expected 120 reached WA, suggesting that 62% of conceived *Tm4sf1* -heterozygous were born live; or, alternatively, (2) Working from Mendelian ratios, about 47% (0.93/2.0) of conceived *Tm4sf1* -heterozygous were born live (Table 1).

Although only 47-62% *Tm4sf1* -heterozygous reached WA, a nearly Mendelian ratio of 1:2:1 (wt:het:ko) was observed at E9.5 to E12.5 Table 1. However, none of the homozygous *Tm4sf1* deficient embryos were viable with a vital heartbeat; see representative movies taken from E9.5 *Tm4sf1* -wild type Movie 1 and Movie 2. *Tm4sf1* knockout embryo does not have a vital heart beat. Brief videos taken from E9.5 embryos show a vital heart beat for the *Tm4sf1* +/+ embryo but not for the *Tm4sf1* -/- embryo. Representative E9.5 embryos further demonstrated that unlike *Tm4sf1* -wild type embryos (Figure 2A (a)), *Tm4sf1* -knockout embryos lacked visible blood vessels in yolk sac and embryo body in bright-field images and lacked *Tm4sf1* positively stained blood vessels in immunofluorescence wholemount (Figure 2A (b)). E10.5 littermates provided further evidence of the inability of *Tm4sf1* -knockout embryos to generate vasculature (Figure S3). A representative mid-sagittal section of a wild type E10.5 embryo revealed that all major vessels stained positively for TM4SF1, as did the cephalic mesenchyme, the condensing mesenchyme in the head (Figure S4).

In accordance with yolk sac genotyping, qPCR performed on total RNA extracted from E9.5 embryos demonstrated the absence of detectable *Tm4sf1* gene expression in the *Tm4sf1* -knockout embryos (Figure 2B (a)). *Tm4sf1* -knockout embryos also were deficient in blood vessel markers including Cd31, Cd144, Tie1, Tie2, VEGFR1 and VEGFR2 (Figure 2B (b)). Expression of TM4SF1 and the six vascular markers in *Tm4sf1* -heterozygous embryos was less than half that in their *Tm4sf1* -wild type littermates (Figure 2B (b)). These differences in vascular gene expression were accompanied by differences in embryo phenotype: Representative E9.5 embryo images from the same litter showed that *Tm4sf1* -heterozygous embryo exhibited smaller body size than their wild type littermate, and the *Tm4sf1* -knockout embryo lacked blood vessels (Figure 2B (b)). Vegfa expression was respectively 6.8-fold and 4.9-fold higher in *Tm4sf1* -knockout and *Tm4sf1* -heterozygous embryos than in wild type embryos (Figure 2B (c)).

Table 1. Genotypes of progeny from TMS4F1-heterozygous intercrosses

	# of embryos (% over total #)									
Age	**+/+**	**+/-a**	**+/-b**	**+/-c**	**-/-**	**Total #**	**litters**	**#/litter**	**viable -/-**	**+/-a: +/+**
E9.5	34 (29.6)	63 (54.8)	0 (0.0)	0 (0.0)	16 (13.9)	113	12	9.4	0	1.85
E10.5	22 (30.1)	41 (56.2)	2 (0.0)	0 (0.0)	10 (13.7)	75	9	8.3	0	1.86
E12.5	33 (34.0)	58 (59.8)	0 (0.0)	0 (0.0)	6 (6.2)§	97	10	9.7	0	1.76
E14.5	25 (39.1)	29 (45.3)	4 (6.3)	2 (3.1)	4 (6.3)§	64	8	8.0	0	1.16
E16.5	27 (40.3)	26 (38.8)	7 (10.4)	1 (1.5)	6 (9.0)§	67	8	8.4	0	0.96
E18.5	34 (39.1)	31 (35.6)	19 (21.8)	3 (3.4)	0 (0.0)	87	11	7.9	0	0.91
WA	80 (51.9)	74 (48.1)	0 (0.0)	0 (0.0)	0 (0.0)	154	30	5.1	0	0.93

Note: E: Embryonic Day; WA: Weaning Age for Genotyping; a: Embryos without Visible Hemorrhagic Blood Vessel or Live at the WA; b: Embryos with Visible Hemorrhagic Brain; c: Necrotic Dead Embryo; §: Embryos were Deteriorating or being Absorbed.

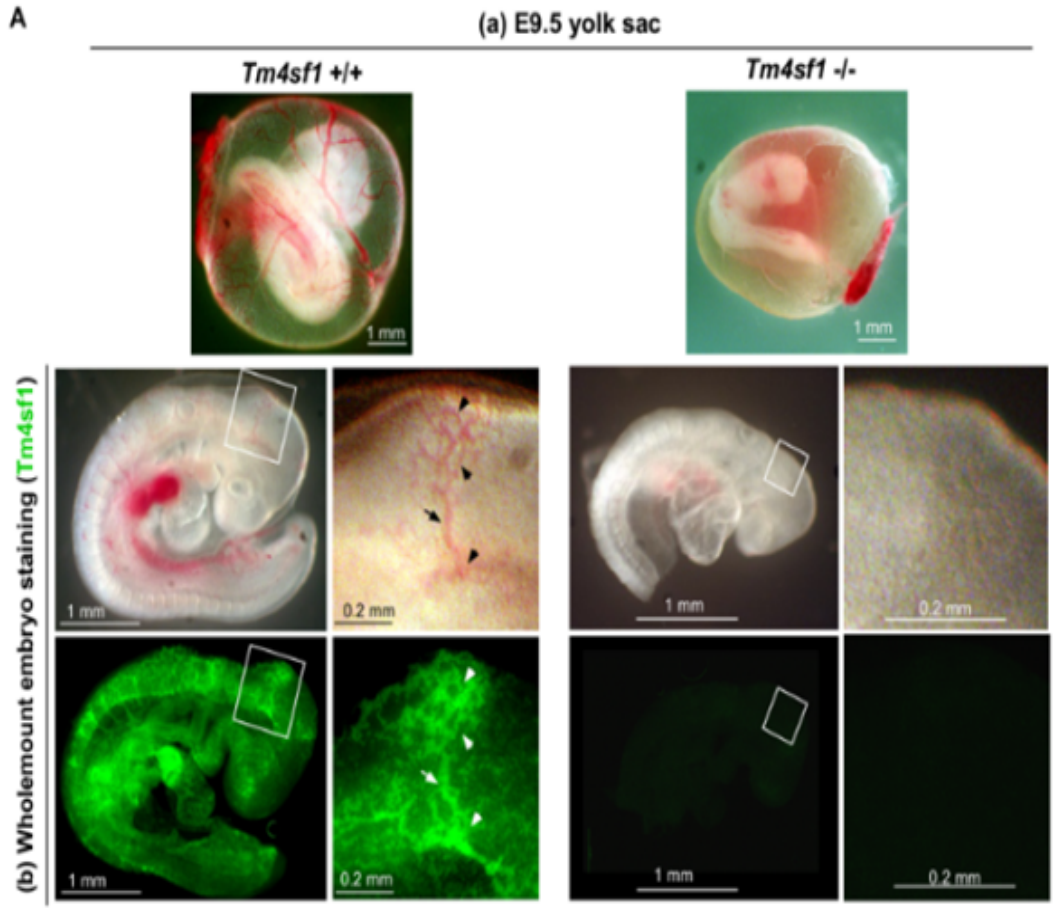

Figure 2A. *Tm4sf1*-knockout mice are embryonically lethal at E9.5. (A) Representative E9.5 bright field embryo images of littermates show developing blood vessels in both (A,a) yolk sac and (A,b) embryo in *Tm4sf1* +/+ but not in *Tm4sf1* -/-. Wholemount embryo staining using Alexa488-conjugated 2A7A demonstrated TM4SF1 protein localization in the *Tm4sf1* +/+ embryo vasculature (white arrows indicate the same locations as the black arrows in bright field images), but no 2A7A staining occurred in the *Tm4sf1* -/- embryo.

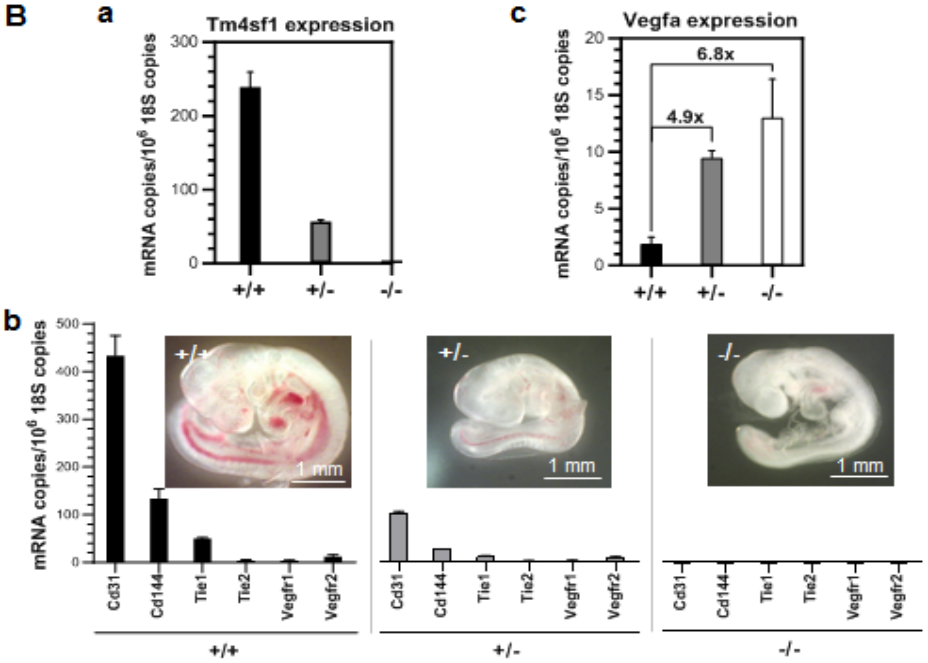

Figure 2B. *Tm4sf1*-knockout embryos fail to develop blood vessels. qPCR was conducted on total RNA prepared from E9.5 littermate embryos (three each of +/+, +/-, and -/- from three different litters). (B,a) Representative RNA quantification demonstrated that *Tm4sf1* -/- embryos, unlike *Tm4sf1* +/+ and +/- embryos, did not express the *Tm4sf1* gene and that (B,b) the known vascular markers Cd31, Cd144, Tie1, Tie2, Vegfr1, and Vegfr2 were also too low to be detected; and, (B,c) in comparison to *Tm4sf1* +/+ embryos, Vegfa expression was at 6.8-fold (p=0.00003) higher in *Tm4sf1* -/- embryos and 4.9-fold (p=0.0014) higher in *Tm4sf1* +/- embryos. (B,b) The representative inset littermate-embryo images show an absence of blood vessels in the -/- embryos, and small body size in the +/- embryo in comparison to the +/+.

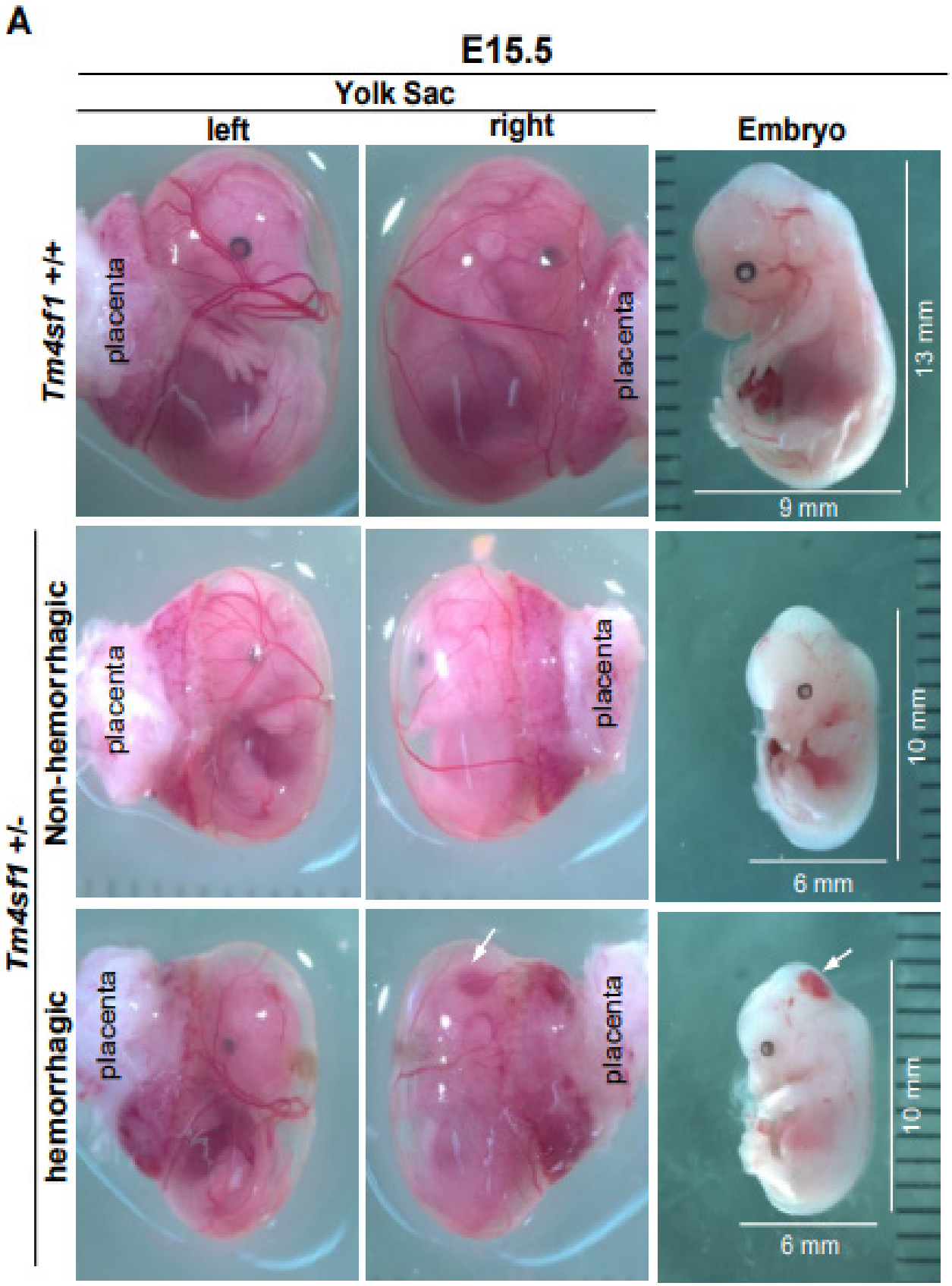

Figure 3A. *Tm4sf1*-heterozygous embryos are smaller in body size and can develop brain hemorrhage. Representative E14.5 *Tm4sf1* +/- embryos had smaller body size than their wild type littermate, and one of the two *Tm4sf1* +/- embryos displayed hemorrhage in the head (white arrows). No obvious hemorrhage appeared in other parts of the embryo body including the yolk sac.

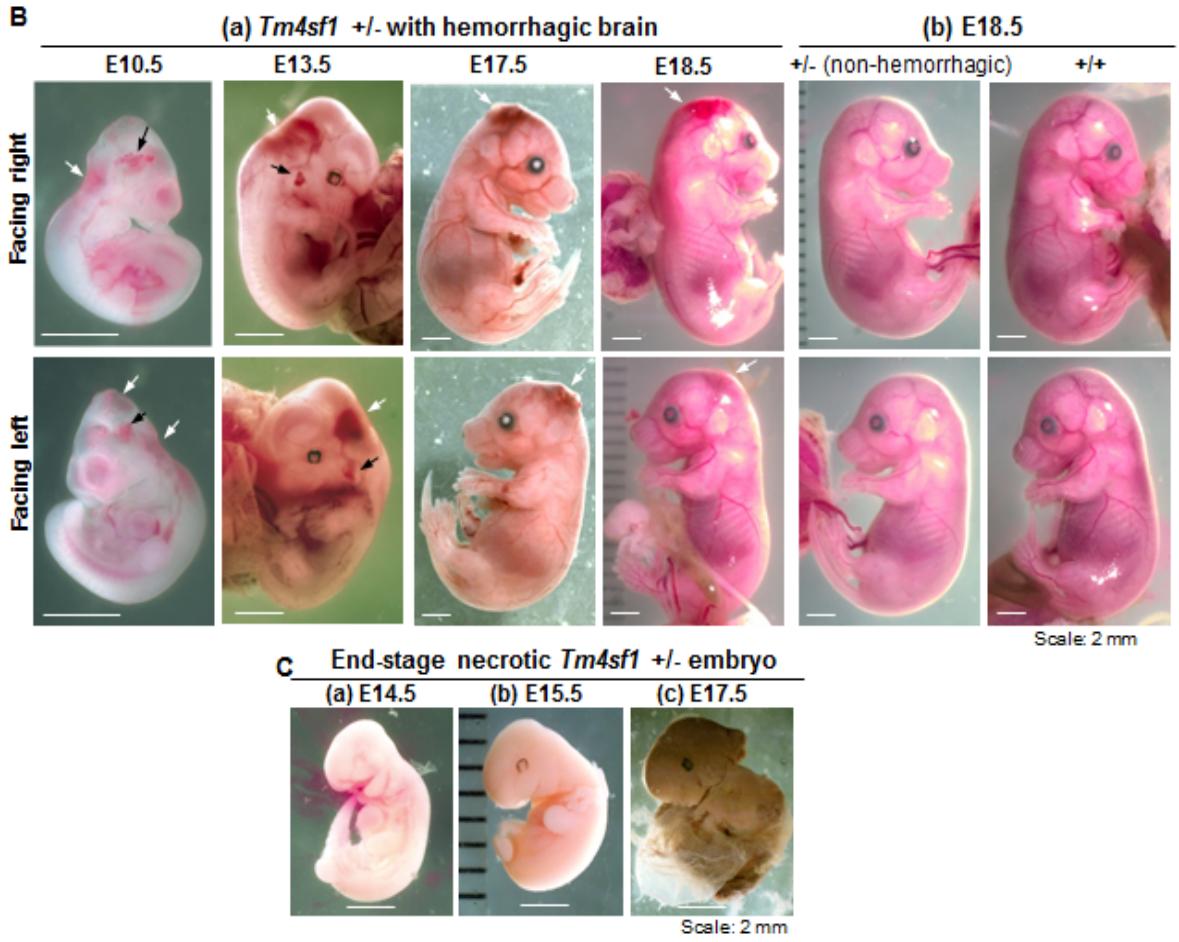

Figure 3B and 3C. *Tm4sf1*-heterozygous embryos can develop lethal brain hemorrhage. (B,a) Representative images from sequential developmental stages of mouse embryos portray brain hemorrhages that occurred in some *Tm4sf1* +/- embryos. The hemorrhage can be seen as early as E10.5 and became more apparent over subsequent days of development (white arrows) with some embryos also showed vascular defect near the jugular vein (black arrows). (B,c) Brain hemorrhages did not affect the embryo growth rate; at E18.5, *Tm4sf1* +/- embryos with and without brain hemorrhage were comparable in body size, and had nearly caught up in size to *Tm4sf1* +/+ embryos. (C) Deceased *Tm4sf1* +/- embryos were noted during embryo harvests at E14.5 (a), E15.5 (b), and E17.5 (c).

Tm4sf1 -heterozygous embryos were smaller in size and approximately half evolved significant brain hemorrhage

Abnormalities of *Tm4sf1* -heterozygous embryos were clearly noted starting about E14.5, when many developed brain hemorrhage (Figure 3; Table S1). Representative E15.5 littermate embryo images reveal *Tm4sf1*-heterozygous displayed smaller body size than their wild type littermate with one of the two *Tm4sf1* -heterozygous exhibiting brain hemorrhage (Figure 3A, white arrow), while other regions of the body including the yolk sac appeared to be normal.

Representative images of developing embryos provide further evidence that visible vascular defects in *Tm4sf1* -heterozygous embryos were largely confined to the head (Figure 3B, white arrow) with some also seen in the vicinity of the jugular vein (Figure 3B, black arrows). Occasionally, some remnants of dead *Tm4sf1* -heterozygous embryos were identified during embryo harvest (Figure 3C). This is consistent with the progressively declining ratio of non-hemorrhagic *Tm4sf1* -heterozygous to wild type embryos from the expected 2:1 Mendelian ratio and observed as 1.16 at E14.5 and 0.91 at E18.5 and 0.93 at WA. These data imply that lethal vascular defects can happen before E18.5 in *Tm4sf1* -heterozygous embryos.

A higher resolution bright field image of a representative E17.5 *Tm4sf1* -heterozygous embryo that exhibited brain hemorrhage demonstrates a lack of integrity in the forebrain-forebrain (fb-fb) and forebrain-midbrain (fb-mb) junctions and an accumulation of blood around the third and fourth ventricles (Figure 4A, c). Transverse H and E section of the hemorrhagic *Tm4sf1* -heterozygous embryo showed that all four ventricles (lateral left and right, third, and fourth) in the head along with the subarachnoid space were filled with blood (Figure 4B, c), but no hemorrhage was observed in the cortex (Figure 4B, c). The *Tm4sf1* -heterozygous littermate without brain hemorrhage resembled wild type embryos and showed normal integrity in the fb-fb and fb-mb regions (Figure 4A, a,b) without blood accumulation in ventricles or subarachnoid space (Figure 4B, a,b).

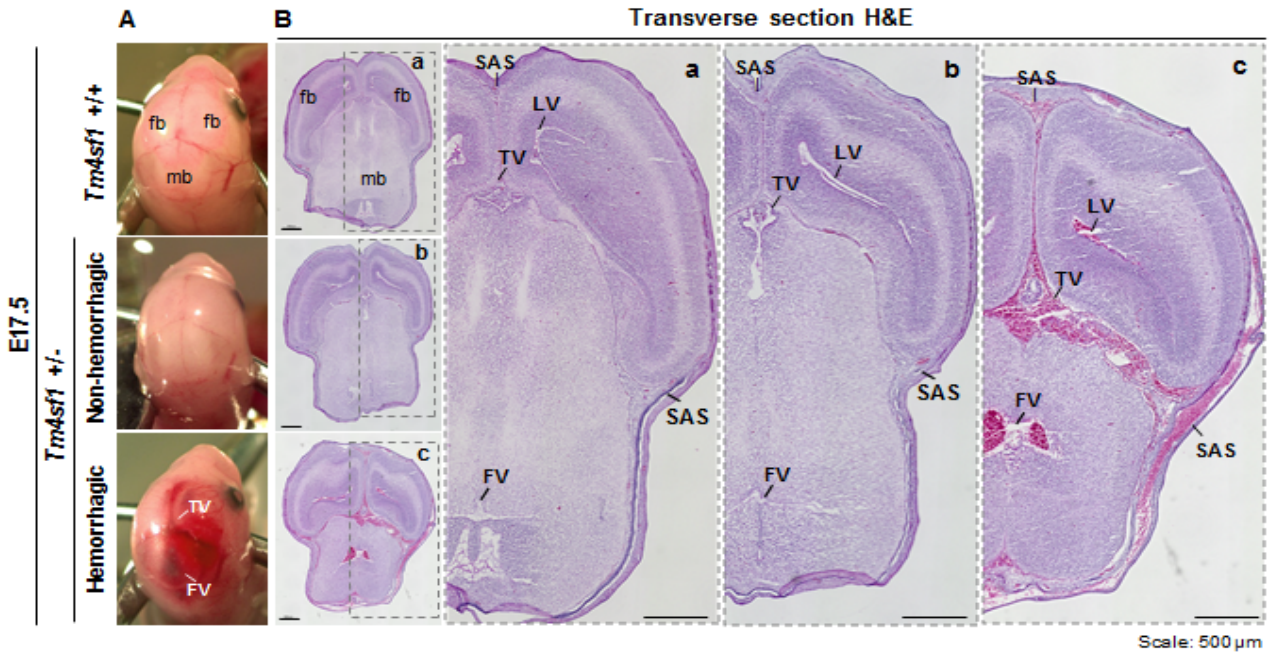

Figure 4. Intracranial hemorrhage in some *Tm4sf1* +/- embryos. Representative bright field head images of E17.5 *Tm4sf1* +/+ and +/- littermates are shown in (A) and their respective transverse H&E histological staining are shown in (B). (A) Lack of integrity in the fb (forebrain)-fb and fb-mb (midbrain) junctions and an accumulation of blood around the TV (third ventricle) and FV (fourth ventricle) were seen in the hemorrhagic *Tm4sf1* +/- embryo (c) but not in the non-hemorrhagic *Tm4sf1* +/- (b) and the *Tm4sf1* +/+ (a) embryos. (B) All four ventricles, TV, FV, and left and right LV (lateral ventricle), and the SAS (subarachnoid spaces) were filled with blood in the hemorrhagic *Tm4sf1* +/- embryo (c) whereas all structures appeared normal in both the non-hemorrhagic *Tm4sf1* +/- (b) and the *Tm4sf1* +/+ (a) embryos.

Whether or not brain hemorrhage was experienced, *Tm4sf1* -heterozygous embryos were smaller in body size at E15.5, but progressively caught up with wild type embryos at later ages, and showed minimal difference in body size at time of birth (Figure 3B, b; Figure S5A). Tracking postnatal growth *via* body weight also demonstrated that *Tm4sf1* -heterozygous and wild type had similar growth rate (Figure S5B), and *Tm4sf1* -heterozygous mice also experienced normal fertility and life-span. The ratio of live born males to females in wild type and in *Tm4sf1* -heterozygous litters were 0.95 and 0.9, respectively (Figure S5C). Overall, the results suggest that the challenging period for mice with deficient TM4SF1 protein expression is during embryonic development, and lethal embryonic brain hemorrhages are equally likely to occur in male and female *Tm4sf1* -heterozygous embryos.

Discussion

Through genetic manipulation approaches, we demonstrate here that *Tm4sf1* null mice experience embryonic lethality by E9.5 due to a failure to form blood vessels, and that the suboptimal level of *Tm4sf1* in *Tm4SF1*-heterozygotes causes smaller body size during early embryonic development with almost half of the embryos experiencing a lethal vascular defect in the head that led to intraventricular and subarachnoid hemorrhage.

Differential expression of TM4SF1 in different vascular beds was observed *in vivo*, with arteries having the highest expression, veins intermediate, and capillaries the lowest (Figure 1). This result was unanticipated since cultured ECs, regardless of their *in vivo* bed of origin, showed uniformly high and similar levels of TM4SF1 expression *in vitro* (Figure S1). We presume that this differential expression is the result of EC interactions with accessory cells to generate distinct vascular beds, [13,14] a process supported by MSC differentiation to smooth muscle cells to form larger vessels like arteries and to pericytes to support veins and capillaries [15]. We exclude the potential involvement of shear stresses as our studies applying laminar (steady, non-turbulent) flow to cultured ECs *via* an orbital shaker did not affect TM4SF1 level (unpublished data).

VEGF-A plays a critical role in EC proliferation for vasculogenesis and angiogenesis through the activation of its receptors expressed on the cell surface [16,17]. Our prior studies demonstrated that, although VEGF-A was supplied in abundance, depletion of TM4SF1 through knockdown [5] resulted in (i) an inability of ECs to perform cytokinesis for proliferation, polarization for movement, or intercellular interactions *in vitro*; and (ii) inhibition of blood vessel maturation in a mouse model of VEGF-A provoked pathological angiogenesis *in vivo*. In a similar manner, high VEGF-A expression failed to avert the avascular nature of E9.5 *Tm4sf1* null embryos (Figure 2). The high VEGF-A expression seen in E9.5 *Tm4sf1* -heterozygous embryos, perhaps caused by hypoxia for urging blood vessel development, may have contributed to ultimate recovery of normal body size in the heterozygous embryos over the course of developmental time (Figure 3B; Figure S5). The smaller embryo body size observed during the *Tm4sf1* -heterozygotes development is not uncommon among knockout mice in which the target gene is involved in blood vessel development; examples include integrin-αvβ8 [18] Erg transcription factor [19] and proteins in the VEGF signaling cascade (Figure 2) [20, 21].

The circulatory system is the first and most essential organ system to begin functioning during embryonic development and is assembled through vasculogenesis and angiogenesis followed by vascular remodeling *via* recruitment of vascular supporting accessory cells [22,23]. Given that TM4SF1 protein expression is specific to the vascular endothelium and the mesenchyme *in vivo* (Figure 1; Figure S4) and cultured cells *in vitro* (Figure S1), TM4SF1 is likely to influence embryonic blood vessel development through both ECs and MSCs. ECs express high levels of VEGFR2/Flk-1 and PDGF-β, and MSCs express high levels of the corresponding ligand VEGF-A and receptor PDGFRβ [24,25] an indication that intimate interactions between the two cell types facilitate blood vessel formation. As yet unpublished studies with cultured ECs show that PLCγ-1, the immediate downstream mediator of VEGFR2/Flk-1 signaling which activates ERK upon Flk-1 activation and produced an embryonic lethal phenotype similar to that of Flk-1 null mice [26] is recruited to TMED. PLCγ-1 is also a downstream mediator of PDGFR in MSC cells [25]. We anticipate that a defect in PLCγ-1 functional activities may be one of the molecular mechanisms underlying the *Tm4sf1* null phenotype. Insufficient TMED-mediated intracellular transport of recruited molecules and/or intercellular interactions in both ECs and MSCs may also contribute to the impairment of vasculogenesis and to the impaired remodeling seen in *Tm4sf1* -heterozygous embryos.

A number of questions remain unanswered: Why was hemorrhage largely limited to the head but no other parts of the *Tm4sf1* -heterozygous embryos? Also, why did hemorrhage happen in only about half of the *Tm4sf1* -heterozygotes, not all? We noted that TM4SF1 protein is highly expressed in the cephalic mesenchyme of E10.5 mouse embryos, with no noticeable

expression in the cortical neuroepithelium. TM4SF1 protein expression is also seen in the choroid plexus epithelium of the lateral ventricle and the subependymal cell layer in adult mouse brains (Figure 1, Figure S3). However, we currently do not have data to elucidate how TM4SF1 expression in these locations influenced the phenotypic development of *Tm4sf1* -heterozygotes. Specifically, we do not know whether the expression in cephalic mesenchyme is transitory, and if differences in TM4SF1 expression regulation in mesenchyme contributed to the occurrence of vascular hemorrhage. We anticipate, based on our occasional observations of end-stage necrosis of *Tm4sf1* -heterozygous embryos as early as E14.5 (Figure 4C), that some *Tm4sf1* -heterozygous embryos may experience lethality before they have developed the apparent intraventricular and subarachnoid hemorrhage seen near birth (Figure 4B). This implies considerable variability among *Tm4sf1* -heterozygous embryos, with some encountering more severe vascular defects with early lethality, others intraventricular and subarachnoid hemorrhage or normal development.

E14.5 is the transition stage from the embryonic to fetal period and is considered to be the most important time point for developmental disorder analyses [27]. In many other perinatally or prenatally lethal mutant mouse lines, half of embryos survive until E14.5, including some in which the cause of death is intracerebral hemorrhage by mutations that affect EC function such as Fli 1 [28] and Erg [19] transcription factors, and *integrin-αvβ8* adhesion molecules [29]. Nonetheless, embryonic intraventricular and subarachnoid hemorrhage has not been reported in studies using genetically manipulated mice including manipulations through the VEGF signaling cascade [20,30,31]. Ventricles are a communicating network of chambers filled with cerebrospinal fluid that in mouse embryos is predominantly produced in the lateral ventricles, is transported through the ventricular system, and enters the subarachnoid space through foramina at the fourth ventricle for final absorbance [32]. In mouse embryos, the lateral (I and II), third, and fourth ventricles develop around E10 and the cerebral aqueduct connecting the third and fourth ventricle is formed and becomes the narrowest part of the cerebrospinal fluid system during late embryonic brain development [32]. We infer that the vascular integrity required to support the ventricles for cerebrospinal fluid clearance is especially challenged by the suboptimal level of TM4SF1 expression.

Future studies, combining proteomic analysis for protein identification with sophisticated spatial biology imaging techniques, possibly aided by knock-in of a reporter gene like lacZ to *Tm4sf1* locus or conditional *Tm4sf1* knockout, will address where and when TM4SF1 is expressed during embryo development, and how it works with recruited proteins for the regulation of blood vessel formation and maturation.

Conclusion

We report that *Tm4sf1* null mouse embryos are avascular and experience lethality at E9.5, while *Tm4sf1* heterozygous embryos are smaller in body size during early embryonic development, and about half die in utero due to an intracranial hemorrhage which becomes apparent in the intraventricular and subarachnoid space by E17.5. Heterozygotes that are born alive appear normal and have no apparent post-natal developmental defects. As noted in our prior reports, TMED form on the cell surface when TM4SF1 is highly expressed and serve as critical signaling mediators through internalization *via* microtubules to the nucleus. This study shows that the timeliness and optimal level of Tm4sf1 expression in endothelial cells and mesenchymal stem cells are of critical importance during embryonic blood vessel development.

Acknowledgement

We thank Dr. Harold F. Dvorak (HFD) for assistance capturing immunohistochemical images of mouse and human organs and for discussions of the manuscript. We thank Dr. William C. Aird and his group for their assistance strategizing the making of TM4SF1-knockout mice, and especially David Beeler who supervised the gene cloning and Katherine Spoke who assisted with ES cell transfection. We thank Andrew Zukauskas for participation in the initial stages of cloning; Dan Li of MGTP core for assistance with quantitative real-time PCR; and transgenic core for the generation of TM4SF1 chimeric mice.

Funding

This work was supported by a BIDMC Chief Academic Officer Pilot Grants (S-C.J.), a NIH grant P01 CA92644 (H.F.D.), by a SIG award RR1S1027990 (H.F.D.), and by a contract from the National Foundation for Cancer Research (H.F.D.).

Competing Interests

The authors declare no competing or financial interests.

Author Contributions

Conceptualization: SCJ; Methodology: CIL, AM, JZ, SCJ; Validation: CIL, AM, JZ, SCJ; Formal analysis: CIL, AM, JZ, SCJ; Investigation: CIL, AM, JZ, SCJ; Resources: CIL, AM, JZ, SCJ; Data curation: CIL, AM, JZ, SCJ; Writing - original draft: SCJ; Writing - review & editing: CIL, AM, HW, JZ, SCJ, HDF; Visualization: CIL, AM, HW, SCJ; Supervision: SCJ; Project administration: SCJ; Funding acquisition: SCJ, HDF.

References

1. Wright, Mark D, Jian Ni and George B Rudy. "The L6 Membrane Proteins-A New Four-Transmembrane Superfamily." *Protein Sci* 9(2000):1594-1600.
2. Hellström, Ingegerd, Paul L Beaumier and Karl Erik Hellström. "Antitumor Effects of L6, an Igg2a Antibody that Reacts with Most Human Carcinomas." *Proc Natl Acad Sci U.S.A* 83(1986): 7059-7063.
3. Denardo, Sally J, Lois F O' Grady, Daniel J Macey and Linda A Kroger, et al. "Quantitative Imaging of Mouse L-6 Monoclonal Antibody in Breast Cancer Patients to Develop a Therapeutic Strategy." *Int J Rad Appl Instrum B* 18(1991): 621-631.
4. Sciuto, Tracey E, Anne Merley, Chi-Iou Lin and Douglas Richardson, et al. "Intracellular Distribution of TM4SF1 and Internalization of TM4SF1-Antibody Complex in Vascular Endothelial Cells." *Biochem Biophys Res Commun* 465(2015): 338-343
5. Shih, Shou-Ching, Andrew Zukauskas, Dan Li and Guanmei Liu, et al. "The L6 Protein TM4SF1 is Critical for Endothelial Cell Function and Tumor Angiogenesis." *Cancer Res* 69(2009): 3272-3277.
6. Zukauskas, Andrew, Anne Merley, Dan Li and Lay-Hong Ang, et al. "TM4SF1: A Tetraspanin-Like Protein Necessary for Nanopodia Formation and Endothelial Cell Migration." *Angiogenesis* 14(2011): 345-354.
7. Lin, Chi-Iou, Anne Merley, Tracey E Sciuto and Dan Li, et al. "TM4SF1: A New Vascular Therapeutic Target in Cancer." *Angiogenesis* 17(2014): 897-907.
8. Lin, Chi-Iou, Chun-Yee Lau, Dan Li, and Shou-Ching Jaminet. "Nanopodia-Thin, Fragile Membrane Projections with Roles in Cell Movement and Intercellular Interactions." *J Vis Exp* 86(2014): e51320.
9. Visintin, Alberto, Kelly Knowlton, Edyta Tyminski and Chi-Iou Lin, et al. "Novel Anti-TM4SF1 Antibody–Drug Conjugates with Activity against Tumor Cells and Tumor Vasculature." *Mol Cancer Ther* 14(2015): 1868-1876.
10. Wada, Youichiro, Dan Li, Anne Merley and Andrew Zukauskas, et al. "A Multi-Gene Transcriptional Profiling Approach to the Discovery of Cell Signature Markers." *Cytotechnology* 63(2011): 25-33.
11. Brown, Lawrence F, Bruce J Dezube, Kathi Tognazzi and Harold F Dvorak, et al. "Expression of Tie1, Tie2, and Angiopoietins 1, 2, and 4 in Kaposi's Sarcoma and Cutaneous Angiosarcoma." *Am J Pathol* 156(2000): 2179-2183.
12. Yuan, Lei, Lauren Janes, David Beeler and Katherine C Spokes, et al. "Role of RNA Splicing in Mediating Lineage-Specific Expression of the Von Willebrand Factor Gene in the Endothelium." *Blood*(2013): 4404-4412.
13. Swift, Matthew R and Brant M. Weinstein. "Arterial–Venous Specification during Development." *Circ Res* 104(2009): 576-588.

14. Beck Jr, Laurence, and Patricia A D'Amore. "Vascular Development: Cellular and Molecular Regulation." *FASEB J* 11(1997): 365-373.

15. Ding, Rubai, Diane C Darland, Michael S Parmacek and Patricia A D'amore, et al. "Endothelial–Mesenchymal Interactions In Vitro Reveal Molecular Mechanisms of Smooth Muscle/Pericyte Differentiation." *Stem Cells Dev* 13(2004): 509-520.

16. Conway, Edward M, Désiré Collen, and Peter Carmeliet. "Molecular Mechanisms of Blood Vessel Growth." *Cardiovasc Res* 49(2001): 507-521.

17. Nagy, Janice A, Sung-Hee Chang, Shou-Ching Shih and Ann M. Dvorak, et al. "Heterogeneity of the Tumor Vasculature." *Semin Thromb Hemost* 36(2010): 321-331.

18. Zhu, Jiangwen, Karin Motejlek, Denan Wang and Keling Zang, et al."β8 Integrins are Required for Vascular Morphogenesis in Mouse Embryos."*Development* 129(2002): 2891-2903.

19. Vijayaraj, Preethi, Alexandra Le Bras, Nora Mitchell and Maiko Kondo, et al. "Erg is a Crucial Regulator of Endocardial-Mesenchymal Transformation during Cardiac Valve Morphogenesis." *Development* 139(2012): 3973-3985.

20. Ferrara, Napoleone, Karen Carver-Moore, Helen Chen and Mary Dowd,et al. "Heterozygous Embryonic Lethality Induced by Targeted Inactivation of the VEGF Gene." *Nature* 380(1996): 439-442

21. Shalaby, Fouad, Jacqueline Ho, William L Stanford and Klaus-Dieter Fischer, et al. "A Requirement for Flk1 In Primitive and Definitive Hematopoiesis and Vasculogenesis." *Cell* 89(1997): 981-990.

22. Risau, Werner. "Mechanisms of Angiogenesis." *Nature* 386(1997): 671-674.

23. Udan, Ryan S., James C. Culver, and Mary E. Dickinson. "Understanding Vascular Development." *Wiley Interdiscip Rev Dev Biol* 2(2013): 327-346.

24. Hellström, Mats, Mattias Kalén, Per Lindahl and Alexandra Abramsson, et al. "Role of PDGF-B and PDGFR-B in Recruitment of Vascular Smooth Muscle Cells and Pericytes during Embryonic Blood Vessel Formation in the Mouse." *Development* 126(1999): 3047-3055

25. Heldin, Carl-Henrik, Åke Wasteson, and Bengt Westermark. "Platelet-Derived Growth Factor." *Mol Cell Endocrinol* 39(1985): 169-187.

26. Liao, Hong-Jun, Tsutomu Kume, Catriona McKay and Ming-Jiang Xu, et al. "Absence of Erythrogenesis and Vasculogenesis in Plcg1-Deficient Mice." *J Biol Chem* 277(2002): 9335-9341.

27. Wilson, Robert, Christina McGuire, Timothy Mohun, and DMDD project. "Deciphering the Mechanisms of Developmental Disorders: Phenotype Analysis of Embryos from Mutant Mouse Lines." *Nucleic Acids Res* 44(2016): D855-D861.

28. Spyropoulos, Demetri D, Pamela N Pharr, Kim R Lavenburg and Pascale Jackers, et al. "Hemorrhage, Impaired Hematopoiesis, and Lethality in Mouse Embryos Carrying aTargeted Disruption of the Fli1 Transcription Factor." *Mol Cell Biol* 20(2000): 5643-5652.

29. McCarty, Joseph H, Rita A Monahan-Earley, Lawrence F Brown and Markus Keller,et al. "Defective Associations Between Blood Vessels and Brain Parenchyma Lead to Cerebral Hemorrhage in Mice Lacking Av Integrins." *Mol Cell Bio* 22(2002): 7667-7677.

30. Carmeliet, Peter, Valérie Ferreira, Georg Breier and Saskia Pollefeyt, et al. "Abnormal blood vessel development and lethality in embryos lacking a single VEGF allele." *Nature* 380(1996): 435-439.

31. Shalaby, Fouad, Janet Rossant, Terry P Yamaguchi and Marina Gertsenstein, et al. "Failure of blood-island formation and vasculogenesis in Flk-1-deficient mice." *Nature* 376(1995): 62-66.

32. Gupta, Ankan, Kevin R Rarick and Ramani Ramchandran. "Established, New and Emerging Concepts in Brain Vascular Development." *Front Physiol* 12(2021): 636736.

How to cite this article: Lin, Chi Iou, Anne Merley, Hiromi Wada and Jianwei Zheng, et al. " TM4SF1 is Essential for Embryonic Blood Vessel Development" *J Blood Lymph* 13(2023):310.